INTERNATIONAL JOURNAL OF REMOTE SENSING, 2017
VOL. 38, NO. 3, 728–741
http://dx.doi.org/10.1080/01431161.2016.1271477

Combining ground-based measurements and MODIS-based spectral vegetation indices to track biomass accumulation in post-fire chaparral

Kellie A. Uyeda [a,b], Douglas A. Stow[c], Dar A. Roberts[d] and Philip J. Riggan[e]

[a]Department of Geography, San Diego State University, San Diego, CA, USA; [b]Department of Geography, University of California, Santa Barbara, CA, USA; [c]Department of Geography, San Diego State University, San Diego, CA, USA; [d]Department of Geography, University of California, Santa Barbara, CA, USA; [e]Pacific Southwest Research Station, United States Forest Service, Riverside, CA, USA

ABSTRACT

Multi-temporal satellite imagery can provide valuable information on the patterns of vegetation growth over large spatial extents and long time periods, but corresponding ground-referenced biomass information is often difficult to acquire, especially at an annual scale. In this study, we test the relationship between annual biomass estimated using shrub growth rings and metrics of seasonal growth derived from Moderate Resolution Imaging Spectroradiometer (MODIS) spectral vegetation indices (SVIs) for a small area of southern California chaparral to evaluate the potential for mapping biomass at larger spatial extents. These SVIs are related to the fraction of photosynthetically active radiation absorbed by the plant canopy, which varies throughout the growing season and is correlated with net primary productivity. The site had most recently burned in 2002, and annual biomass accumulation measurements were available from years 5 to 11 post-fire. We tested the metrics of seasonal growth using six SVIs: normalized difference vegetation index (NDVI), enhanced vegetation index (EVI), soil adjusted vegetation index (SAVI), normalized difference water index (NDWI), normalized difference infrared index 6 (NDII6), and vegetation atmospherically resistant index (VARI). Several of the seasonal growth metrics/SVI combinations exhibit a very strong relationship with annual biomass, and all SVIs show a strong relationship with annual biomass (R^2 for base value time series metric ranging from 0.45 to 0.89). Although additional research is required to determine which of these metrics and SVIs are the most promising over larger spatial extents, this approach shows potential for mapping early post-fire biomass accumulation in chaparral at regional scales.

ARTICLE HISTORY
Received 27 June 2016
Accepted 3 December 2016

1. Introduction

Wildfires in chaparral commonly occur over vast expanses of land (Keane et al. 2008). While vegetation recovery typically occurs rapidly in the first two decades following a fire (Keeley and Keeley 1981; McMichael et al. 2004), the recovery process is spatially

CONTACT Kellie A. Uyeda kellie.uyeda@gmail.com Department of Geography,San Diego State University, 5500 Campanile Drive, San Diego, CA, 92182-4493

variable (Kinoshita and Hogue 2011). Remotely sensed imagery provides a spatially comprehensive view of the post-fire recovery process. Recent studies have used multi-temporal imagery from sources such as Landsat Thematic Mapper/Enhanced Thematic Mapper Plus (Hope, Tague, and Clark 2007), Advanced Visible/Infrared Imaging Spectrometer (AVIRIS) (Riano et al. 2002), and Aqua/Terra Moderate Resolution Imaging Spectroradiometer (MODIS) (Kinoshita and Hogue 2011) to study post-fire recovery in chaparral. MODIS data, in particular, provide an excellent opportunity to study post-fire recovery because processed temporal composite data sets are available with high temporal resolution (8 or 16 days, depending on the product) dating back to 2000. Spectral vegetation index (SVI) products such as the normalized difference vegetation index (NDVI) are generated from radiometrically calibrated, atmospherically corrected, and geometrically processed MODIS data. NDVI and related SVIs are related to vegetation properties such as biomass, canopy structure, chlorophyll content, and potential photosynthetic activity (Gamon et al. 1995; Huete et al. 2002). The relatively high temporal resolution allows researchers to study the properties of recovery throughout the entire growing season, rather than at just one or a few times of the year. Seasonal growth metrics based on the full SVI time series provide detailed information about vegetation recovery (van Leeuwen et al. 2010).

Previously, studies of multi-temporal satellite image analyses of chaparral growth following fire have been based on chronosequence approaches to sampling SVI values (e.g. NDVI, NDVI-derived leaf area index, and green vegetation fraction) across landscapes (Henry and Hope 1998; McMichael et al. 2004; Peterson and Stow 2003). In a chronosequence approach, space is substituted for time, such that the SVI values are sampled from different age stands to create an SVI time trajectory. While this approach allows for only one or a few well-processed images to be used to generate trajectories, some shortcomings are that it does not account for variability related to precipitation (Uyeda, Stow, and Riggan 2015) and might miss variability within single age stands, which can be substantial (Uyeda et al. 2016a).

Although remote-sensing studies provide valuable information on post-fire recovery, deriving accurate biomass measurements from remotely sensed data is difficult (Lu 2006), and many studies of post-fire recovery either don't include field data (Kinoshita and Hogue 2011) or provide only cover data (van Leeuwen et al. 2010). The lack of accurate biomass and biomass accumulation measurements is an important limitation in studying post-fire recovery (Uyeda, Stow, and Riggan 2015).

Previous studies have found a strong correlation between tree ring width and estimates of net primary productivity based on NDVI data in boreal forests (Malmström et al. 1997) and with tree ring width and integrated NDVI in the central Great Plains (Wang et al. 2004). Annual changes in oak tree circumference measured over a ten-year period were strongly correlated with integrated annual enhanced vegetation index (EVI) (Garbulsky et al. 2013). These studies provide evidence of strong relationships between satellite-based measures of annual growth and field-based metrics in mature forested areas, although it is not yet known whether strong relationships exist for post-fire shrublands.

In a previous study, we examined the relationship between shrub fractional cover measured using high spatial resolution colour infrared imagery and MODIS NDVI for several chaparral stands in the first two decades of post-fire recovery (Uyeda, Stow, and

Riggan 2015). We found that tracking a single stand through time revealed important details on the recovery process compared with the chronosequence approach. However, an important limitation of the study was the lack of field-measured biomass data. In another earlier work, we found that the use of shrub growth rings and regression equations relating shrub biomass to stem basal area can be an effective method for estimating biomass accumulation in the early years of post-fire chaparral recovery (Uyeda et al. 2016b).

In this study, we expand on these earlier works to compare the annual biomass accumulation measured using shrub growth rings with MODIS-based metrics of vegetation growth in a seven-year post-fire recovery period in chaparral shrublands. We test several metrics of annual growth from multiple SVIs to address the following research questions: 1) which MODIS-based metrics of annual growth are the most closely related to ground-based measurements of annual biomass accumulation in chaparral obligate seeder shrubs and what is the degree of temporal co-variability?; and 2) is the relationship between MODIS-based growth metrics and biomass sufficiently strong to indicate a potential for mapping biomass growth at regional scales?

2. Methods

2.1. *Study site*

The San Dimas Experimental Forest (SDEF) is a research site managed by the US Forest Service located in the San Gabriel Mountains in Los Angeles County, CA, USA. It is predominantly covered by mixed chaparral vegetation, with coastal sage scrub, oak woodland, and mixed conifers also present. The obligate seeding species *Ceanothus crassifolius* is common on south-facing slopes, and *Ceanothus oliganthus*, another obligate seeder, is common on north-facing slopes. *Quercus berberidifolia*, an obligate resprouter, is also found occasionally on north-facing slopes and *Adenostoma fasciculatum*, a facultative seeder, is found in low abundance throughout SDEF. The entire study site burned in September 2002. This area experiences a Mediterranean-type climate, with hot dry summers and cool wet winters. Average precipitation for the area is approximately 720 mm (http://www.prism.oregonstate.edu/, accessed 4 April 2014).

2.2. *Fieldwork*

The full details of the field sampling methods are provided in Uyeda et al. (2016b). Field plots were located within two 6.25 ha areas (250 m by 250 m) within 500 m of one another. We established three randomly located replicate plots, each 16 m^2 (4 m x 4 m), stratified by aspect (north, south, east, west), in each of the two 6.25 ha study areas. This resulted in 12 original plots per study area and a total of 24 for the entire site. At each plot, we measured all stem diameters at the height of 4 cm and collected stem cross sections from five randomly selected *Ceanothus spp*. shrubs. Five plots had fewer than three cross sections of suitable quality and were removed from the analysis, resulting in a final number of nine plots in the northern study area and 10 in the southern study area (Figure 1). It was difficult to determine the ring position in stems smaller than approximately 1 cm, and multiple small stems were randomly selected in some plots. Other

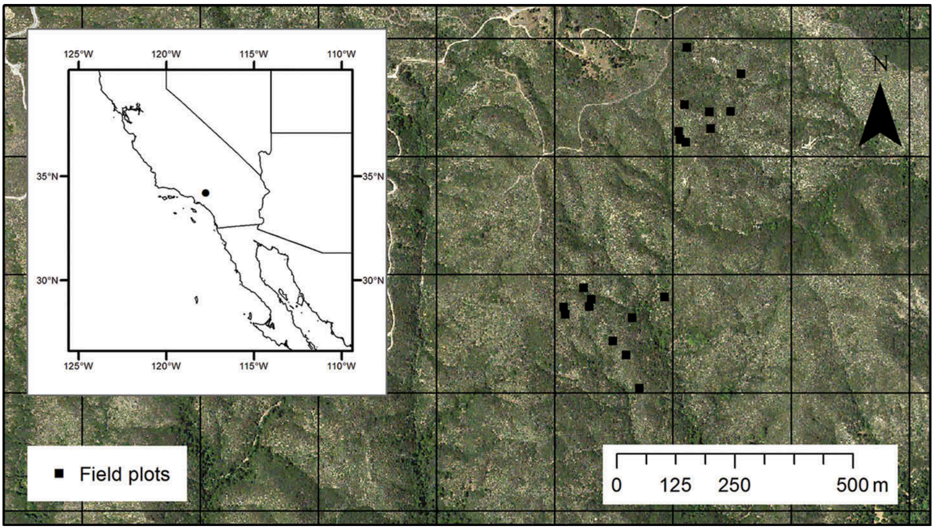

Figure 1. Field site in san Dimas Experimental Forest, Los Angeles County, California. Gridlines show the nominal MODIS MOD13Q1 footprint boundaries. The coordinates of the field site are approximately 34.198551 (N) −117.758572 (W).

stems had insect damage, which obscured the rings. All plot sampling took place in the autumn of 2013.

Species-specific regression equations relating stem diameters to dry shrub biomass were calculated from the destructive sampling of shrubs that took place during the autumn 2013 sampling, as well as from nearby sampling from autumn 2011 and spring 2012. A close relationship between stem diameter and dry shrub biomass was found for these sampled shrubs, with coefficient of determination (R^2) values ranging from 0.79 to 0.98 (Uyeda et al. 2016b).

The stem cross sections were sanded with progressively finer sandpaper up to 400 grit and photographed using a flat platform and stationary camera. We then measured the growth ring diameters along the maximum and minimum axes of each cross section using ImageJ software (Abràmoff, Magalhães, and Ram 2004).

We calculated the basal area for each year of growth using the mean of the maximum and minimum diameter measurements. Each year of growth was then converted to a percentage of the total area (representing growth at the end of 2013), and the mean percentage increment in basal area was calculated for each plot. We assumed that the bark width was a constant ratio of the total stem diameter (Bush and Brand 2008), and therefore used the inside bark measurements to calculate the percentage increment values. We applied the average plot-level percentage increment to all live stems measured in each plot to estimate what the basal area would have been in each year. The annual plot-level biomass increment was then calculated for each year post-fire using the previously described regression equations. Next, we calculated the average of the annual growth increment for each of the two study areas. Due to problems with interpreting the smallest growth rings on some of the shrubs, we started the analysis at the fourth year of recovery. This means that annual changes in biomass data are available for years 5–11 after the fire. Although dendrochronological studies typically use standardized growth ring widths to account for the decline in ring width age (Fritts and Swetnam 1989), in this study we used the total area values because we related stem area directly to plot-level biomass increment.

2.3. *Image processing*

The MODIS MOD13Q1 vegetation index and the MCD43A4 nadir bidirectional reflectance distribution function (BRDF) products for tile h08v05 were downloaded from the Land Processes Distributed Active Archive for the dates starting from February 2000 to 2013. All image data sets were reprojected from Sinusoidal to Universal Transverse Mercator projections, then subset to the study area. Using the MODIS vegetation index product (MOD13Q1), we created a time series of NDVI and EVI from February 2000 to December 2013 for the two pixels whose ground resolution elements encompass the study sites. The MOD13Q1 product is corrected for atmospheric and illumination effects, has a spatial resolution of 250 m, and is produced using 16 day composite periods.

We also calculated SVIs using the MODIS nadir BRDF adjusted reflectance product (MCD43A4) for the two pixels covering the study sites. The MCD43A4 product has a spatial resolution of 500 m and is produced using 8 day composite periods. The SVIs calculated from this product include NDVI, EVI, soil adjusted vegetation index (SAVI), normalized difference water index (NDWI), normalized difference infrared index 6 (NDII6), and vegetation atmospherically resistant index (VARI). Equations for each SVI are given in Table 1.

All the time series were smoothed using the Savitzky–Golay filtering algorithm and gap-filled to remove low-quality data using TIMESAT software (Chen et al. 2004; Jonsson and Eklundh 2004). The TIMESAT parameters used were Savitzky–Golay half window size of four time periods, adaptation strength of two, spike removal based on median filtering with a spike value of one, an envelope iteration value of two, and seasonal start/end thresholds of 10% of the amplitude as measured from the minimum values at the start and end of each season. We used the pixel reliability summary layer and gave high-quality data full weighting, marginal data half weight, and cloudy pixels zero weight. For each of the seven growing seasons and each SVI (NDVI, EVI, SAVI, NDWI, NDII6, and VARI), we output several of the growth metrics calculated in TIMESAT. These metrics include the maximum (the highest smoothed value observed during the growing season), base value (the average of the minimum values from the beginning and end of the growing season), amplitude (difference between the maximum and base value),

Table 1. Equations for each spectral vegetation index.

Spectral Vegetation Index	Equation	Reference
NDVI	$\frac{\rho_2-\rho_1}{\rho_2+\rho_1}$	(Rouse et al. 1973)
EVI	$2.5\times\frac{\rho_2-\rho_1}{\rho_2+6\times\rho_1-7.5\times\rho_3+1}$	(Huete et al. 2002)
SAVI	$\frac{\rho_2-\rho_1}{\rho_2+\rho_1+0.5}\times(1+0.5)$	(Huete 1988)
NDWI	$\frac{\rho_2-\rho_5}{\rho_2+\rho_5}$	(Gao 1996)
NDII6	$\frac{\rho_2-\rho_6}{\rho_2+\rho_6}$	(Hunt and Rock 1989)
VARI	$\frac{\rho_4-\rho_1}{\rho_4+\rho_1-\rho_3}$	(Gitelson et al. 2002)

Subscripts correspond to MODIS band numbers (band 1 = 620–670 nm; band 2 = 841–876 nm; band 3 = 459–479 nm; band 4 = 545–565 nm; band 5 = 1230–1250 nm; band 6 = 1628–1652 nm). ρ = reflectance.

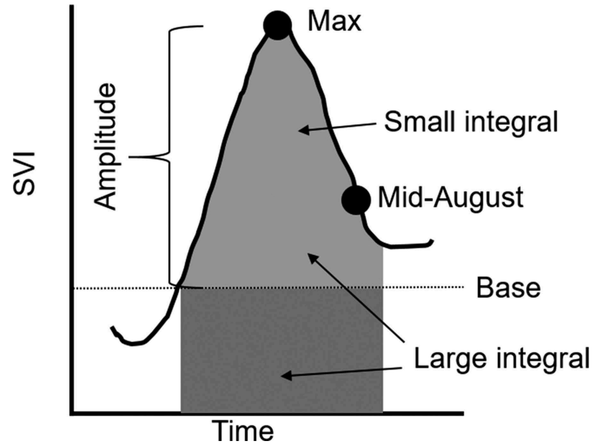

Figure 2. Seasonal growth metrics, illustrated with NDVI data for the 2008–2009 growing season. The maximum and base values are indicated with horizontal lines. The amplitude is the difference of these values. The large integral is the total area under the curve (all shaded area) and the small integral is the area between the base value and the growth curve (lighter shaded area).

and the small and large integrals of the seasonal growth curve (small is the area between the growth curve and the base value, large is the total area below the growth curve) (Figure 2). In addition, we selected the unsmoothed SVI observed in mid-August of each year.

Of these annual TIMESAT metrics, the maximum value may be a useful metric because it is related to the seasonal peak vegetation levels: however, in post-fire chaparral, this maximum value might actually represent high NIR reflectance contributions from herbaceous annual vegetation that thrives during the wet winter and spring, but dies back by summer. The base value is likely a better metric to capture the levels of evergreen shrub vegetation, since it should not be impacted by herbaceous plants. The amplitude provides a metric of seasonal growth, which might reflect the growth patterns of herbaceous plants, especially in the early years of recovery. The small integral provides a metric of seasonal growth throughout the season relative to the summer/autumn time period when only evergreen shrubs are present. The large integral is related to total vegetation growth throughout the season (Jonsson and Eklundh 2004). The August value is similar to the base value in that it incorporates only evergreen, rather than herbaceous, vegetation. However, this metric varies from the base value in that it does not include the value from the beginning of the season, making it perhaps more sensitive to the actual levels of evergreen shrub vegetation at the end of each season.

2.4. *Data analysis*

We conducted a series of bivariate regressions of the SVI seasonal metrics against stand-level biomass. We exhaustively tested the relationships between the growth metrics (maximum, base value, amplitude, small integral, large integral, mid-August value) for each of the SVIs against the field measures of biomass determined from growth ring analysis for years 5–11 post-fire (n = 7). All statistical analyses were conducted using the R statistical software package.

3. Results

The overall patterns of the time series generated from the six SVIs are similar (Figure 3). All show a sharp decline corresponding to the 2002 wildfire, and a period of rapid recovery in the first few years following the fire. Recovery continues steadily throughout the study period, although the final SVI levels remain lower than the pre-fire conditions.

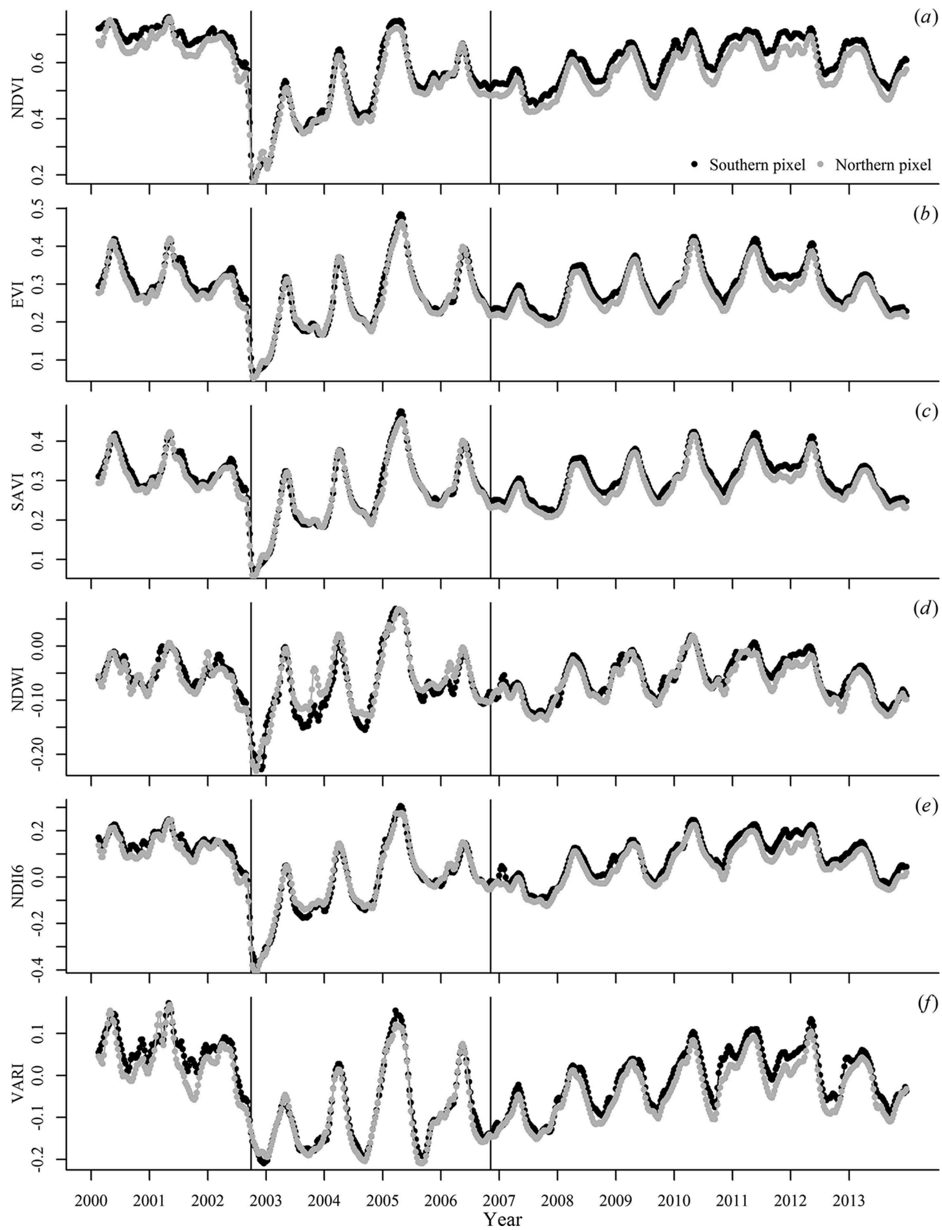

Figure 3. Time series of (*a*) NDVI, (*b*) EVI, (*c*) SAVI (*d*) NDWI, (*e*) NDII6, and (*f*) VARI for the northern and southern pixels generated from the MCD43A4 MODIS product. Vertical lines indicate the date of fire (fall 2002) and the start of the field-based biomass time series (fall 2006).

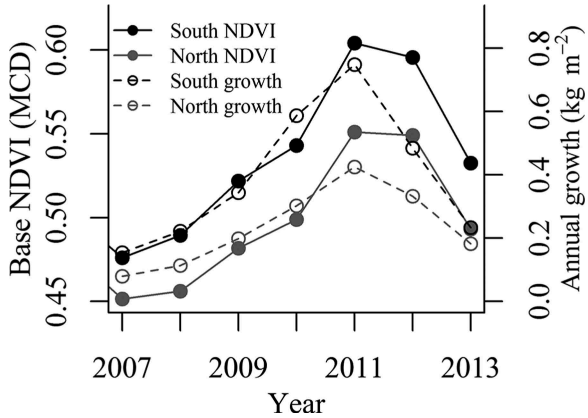

Figure 4. Base NDVI and annual growth for the northern and southern study areas.

The final year of growth (2012–2013 growing season) is somewhat lower than the several previous years, but this is likely due to low precipitation in this year (Uyeda et al. 2016b). The SVI values tend to be lower for the northern study area compared with the southern study area (Figure 3). This corresponds to the pattern of slightly lower biomass values observed in the northern study area (Figure 4).

The base value for many of the SVIs tracks closely with annual biomass increment, with the coefficient of determination (R^2) values ranging from 0.45 to 0.89 (Figure 5, Table 2, n = 7). The maximum value also shows a close relationship with biomass, with the R^2 values ranging from 0.46 to 0.84. The large integral tends to have somewhat lower R^2 values, with a range of 0.28–0.92. The small integral is only significant ($p < 0.01$) for one SVI, and the amplitude is not significant for any of the SVIs tested. The August

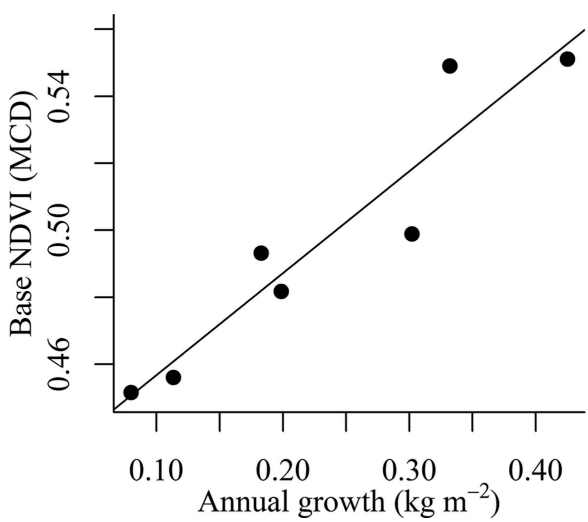

Figure 5. Regression of annual growth and base NDVI for the northern study area. R^2 = 0.89; p = 0.001.

Table 2. Regression results for each seasonal metric and annual biomass increment from the two study areas (n = 7).

	Northern study area									
	Maximum		Base		Amplitude		Large integral		Small integral	
	R^2	p	R^2	p	R^2	p	R^2	p	R^2	p
NDVI (MOD)	0.57	0.049	**0.79**	**0.008**	0.04	0.660	0.46	0.093	0.23	0.273
NDVI (MCD)	**0.77**	**0.009**	**0.89**	**0.001**	0.12	0.444	0.66	0.027	0.42	0.118
EVI (MOD)	0.57	0.048	**0.85**	**0.003**	0.25	0.258	0.60	0.042	0.40	0.130
EVI (MCD)	**0.74**	**0.013**	**0.86**	**0.003**	0.37	0.150	0.47	0.089	0.20	0.311
SAVI	**0.74**	**0.013**	**0.86**	**0.003**	0.34	0.170	0.47	0.087	0.20	0.311
NDWI	0.46	0.095	**0.82**	**0.005**	0.10	0.480	0.44	0.104	0.33	0.177
NDII6	**0.73**	**0.014**	**0.77**	**0.009**	0.18	0.340	**0.83**	**0.004**	0.36	0.156
VARI	**0.83**	**0.004**	**0.80**	**0.007**	0.68	0.022	**0.90**	**0.001**	**0.81**	**0.006**
	Southern study area									
	Maximum		Base		Amplitude		Large integral		Small integral	
	R^2	p	R^2	p	R^2	p	R^2	p	R^2	p
NDVI (MOD)	0.64	0.030	0.65	0.029	0.10	0.482	0.42	0.118	0.36	0.155
NDVI (MCD)	0.66	0.027	**0.73**	**0.014**	0.00	0.911	0.28	0.218	0.18	0.344
EVI (MOD)	0.65	0.028	**0.76**	**0.010**	0.16	0.369	0.59	0.045	0.56	0.052
EVI (MCD)	**0.84**	**0.004**	0.68	0.023	0.53	0.064	0.68	0.022	0.29	0.217
SAVI	**0.83**	**0.004**	0.68	0.023	0.51	0.070	**0.74**	**0.013**	0.34	0.171
NDWI	0.73	0.015	**0.87**	**0.002**	0.09	0.504	**0.92**	**0.001**	0.22	0.293
NDII6	0.69	0.021	0.45	0.098	0.28	0.224	0.73	0.015	0.43	0.112
VARI	0.68	0.022	0.59	0.044	0.50	0.078	0.70	0.019	**0.80**	**0.007**

Spectral vegetation indices tested include normalized difference vegetation index calculated using MOD13Q1 (NDVI (MOD)) and calculated using MCD43A4 (NDVI (MCD)), enhanced vegetation index calculated using MOD13Q1 (EVI (MOD)) and using MCD43A4 (EVI (MCD), soil adjusted vegetation index (SAVI), normalized difference water index (NDWI), normalized difference infrared index 6 (NDII6), and vegetation atmospherically resistant index (VARI). SAVI, NDWI, NDII6, and VARI were calculated using MCD43A4. Bold text indicates that regression results are significant at p = 0.01.

values also track closely with the annual biomass increment, with R^2 values of 0.56–0.89 (Table 3).

In terms of individual SVI comparisons, there are a couple of noteworthy patterns. Although most SVIs have significant results ($p < 0.01$) for the base and maximum metrics (particularly in the northern study area), the VARI regressions are significant at the

Table 3. Regression results for August SVIs and annual biomass increment from the two study areas (n = 7).

	North		South	
	R^2	p	R^2	p
NDVI (MOD)	0.69	0.021	0.64	0.031
NDVI (MCD)	**0.85**	**0.003**	**0.84**	**0.004**
EVI (MOD)	0.56	0.053	**0.78**	**0.009**
EVI (MCD)	0.68	0.022	**0.83**	**0.004**
SAVI	0.70	0.018	**0.84**	**0.003**
NDWI	0.51	0.073	**0.81**	**0.006**
NDII6	**0.80**	**0.006**	**0.89**	**0.001**
VARI	**0.73**	**0.014**	**0.73**	**0.014**

Spectral vegetation indices tested include normalized difference vegetation index calculated using MOD13Q1 (NDVI (MOD)) and calculated using MCD43A4 (NDVI (MCD)), enhanced vegetation index calculated using MOD13Q1 (EVI (MOD)) and using MCD43A4 (EVI (MCD), soil adjusted vegetation index (SAVI), normalized difference water index (NDWI), normalized difference infrared index 6 (NDII6), and vegetation atmospherically resistant index (VARI). SAVI, NDWI, NDII6, and VARI were calculated using MCD43A4. Bold text indicates that the regression results are significant at p = 0.01.

$p \leq 0.05$ level for every metric in the northern study area, and nearly every metric in the southern study area. The SVIs generated from the BRDF corrected MCD43A4 MODIS product tend to yield higher R^2 values than the equivalent SVIs from the MOD13Q1 MODIS product.

4. Discussion

In this study, we explored the temporal co-variability between ground-based measurements of annual chaparral growth and MODIS-based seasonal growth metrics for the fourth to eleventh year following burning by a wildfire. We found that up to 92% of the variance in MODIS growth metrics can be explained by annual biomass growth. This strong relationship indicates that this integrated field-satellite measurement and scaling approach is sufficiently promising to further develop and implement for mapping chaparral (and likely other shrublands) biomass growth at regional scales. The success of scaling from field to regional scales could likely be improved further by classifying shrubs by growth form using high spatial resolution imagery (Schmidt et al. 2016).

The variation in SVI values throughout the growing season track with seasonal patterns of live fuel moisture (LFM), which is related to the timing and quantity of annual precipitation (Dennison, Moritz, and Taylor 2008). The SVIs examined in this study are well known to track with LFM, particularly during the annual 'dry down' period during the summer drought (Peterson, Roberts, and Dennison 2008). In particular, VARI has been shown to have a close relationship with field-measured LFM (Stow, Niphadkar, and Kaiser 2005).

Although the base value time series metric closely co-varies with biomass for many of the SVIs examined, the August SVIs showed similar close relationships. This is noteworthy because the data-processing requirements for single date per year SVIs are much reduced when compared with the full temporal resolution of 46 images per year (for the 8 day MODIS products). It is not surprising that amplitude and small integral values are not closely related to annual biomass growth, as these metrics are more closely related to the herbaceous vegetation component. We expected the large integral to be more closely related to shrub growth, as this metric is related to total productivity. However, it is possible that the herbaceous component still present at this phase of recovery contributed to the SVIs summed to calculate the large integral, resulting in a pattern distinct from that of shrub recovery. Whereas shrubs recover quickly in the years following a fire, herbaceous cover can remain relatively high in the early post-fire years (Keeley, Fotheringham, and Baer-Keeley 2005), possibly contributing to the total productivity signal of MODIS SVI trajectories.

Although the results of this study indicate that the base and August values are closely related to annual growth for nearly all of the SVIs examined, it is more difficult to identify the most promising SVI based on only two study areas (and two associated MODIS pixels). The SVI with the highest R^2 value for a given seasonal metric in the northern study area is not necessarily the SVI with the highest value in the southern area. It would be necessary to extend the study over larger areas in order to determine the optimal SVI, which would require substantial field personnel resources and effort. When extending this work over a larger area, it might also be desirable to aggregate the MODIS pixels to a coarser resolution to reduce the effects of gridding artefacts in the satellite imagery. These gridding artefacts include geolocation and 'pixel shift' errors (mismatch between the predetermined grid and the actual location sampled) (Tan et al. 2006).

Another area for further research is to determine how the relationship between SVIs and biomass changes as the stands reach maturity. Based on the growth trajectories measured in previous studies, the biomass values measured at 11 years old are likely to at least double over the following decade of post-fire recovery (Riggan et al. 1988; Uyeda et al. 2016b). The rate of biomass accumulation typically declines with time within the first two decades of recovery, but there appears to be positive net accumulation at least until an age of approximately 40 years (Rundel and Parsons 1979; Black 1987). NDVI in particular is prone to saturate at high biomass values, although not necessarily in chaparral (Huete et al. 2002). As the rate of biomass accumulation declines and SVIs possibly reach an asymptote in mature stands, the overall relationship is likely to change.

Patterns of biomass growth are important for understanding issues such as ecosystem health and fuel loading. Chaparral subject to frequent fires is prone to type conversion, resulting in sub-shrubs or grasses in areas once dominated by dense shrubs (Lippitt et al. 2012). Climate change is also likely to change the patterns of productivity. The results of field (Prieto et al. 2009) and modelling (Tague, Seaby, and Hope 2009) studies suggest that productivity in Mediterranean-type climate shrublands could be reduced in a warmer climate as greater water stress is placed on plants. However, a warmer climate combined with greater concentrations of CO_2 could increase chaparral productivity (Tague, Seaby, and Hope 2009). It is not yet clear how these potential changes in productivity will change fuel accumulation and, ultimately, fire patterns. This study shows that there is strong potential for using the combination of remotely sensed imagery and shrub growth rings to measure the annual changes in biomass accurately across large spatial scales, which could be used to monitor ecosystem recovery and change through time.

Acknowledgements

Mike Oxford from the USFS arranged for access to SDEF. I. Schmidt, Y. Granovskaya, J. McCullough, K. Walsh, A. Clark, J. Schichtel, L. Handa, M. Hartfelder, K. Hartfelder, E. Storey, R. Elliott, and A. Lewis provided assistance with field vegetation sampling. Funding for this project was provided by the USDA Forest Service through American Recovery and Reinvestment Act Agreement No. 10-JV-11279701-10: 'Airborne remote sensing to enable hazardous fuels reduction, forest health protection, rehabilitation and hazard mitigation activities on Federal lands', Dr Philip Riggan, Principal Investigator.

Disclosure statement

No potential conflict of interest was reported by the authors.

Funding

Funding for this project was provided by the USDA Forest Service through American Recovery and Reinvestment Act Agreement No. 10-JV-11279701-10: 'Airborne remote sensing to enable hazardous fuels reduction, forest health protection, rehabilitation and hazard mitigation activities on Federal lands', Dr. Philip Riggan, Principal Investigator.

ORCID

Kellie A. Uyeda http://orcid.org/0000-0001-7043-3870

References

Abràmoff, M. D., P. J. Magalhães, and S. J. Ram. 2004. "Image Processing with ImageJ." *Biophotonics International* 11 (7): 36–41. doi:10.1117/1.3589100.

Black, C. H. 1987. "Biomass, Nitrogen, and Phosphorus Accumulation over a Southern California Fire Cycle Chronosequence." In *Plant Response to Stress - Functional Analysis in Mediterranean Ecosystems*, edited by J. D. Tenhunen, F. M. Catarino, O. L. Lange, and W. C. Oechel, 445–458. Springer. http://e-collection.library.ethz.ch/eserv/eth:6925/eth-6925-01.pdf?pid=eth:6925&dsID=eth-6925-01.pdf.

Bush, R., and G. Brand. 2008. *Lake States (LS) Variant Overview - Forest Vegetation Simulator. Internal Report*. Coloroda: Fort Collins.

Chen, J., P. Jönsson, M. Tamura, Z. Gu, B. Matsushita, and L. Eklundh. 2004. "A Simple Method for Reconstructing A High-Quality NDVI Time-Series Data Set Based on the Savitzky-Golay Filter." *Remote Sensing of Environment* 91 (3–4): 332–344. doi:10.1016/j.rse.2004.03.014.

Dennison, P. E., M. A. Moritz, and R. S. Taylor. 2008. "Evaluating Predictive Models of Critical Live Fuel Moisture in the Santa Monica Mountains, California." *International Journal of Wildland Fire* 17: 18–27. doi:10.1071/WF07017.

Fritts, H. C., and T. W. Swetnam. 1989. "Dendroecology: A Tool for Evaluating Variations in past and Present Forest Environments." *Advances in Ecological Research* 19 (C): 111–188. doi:10.1016/S0065-2504(08)60158-0.

Gamon, J. A., C. B. Field, M. L. Goulden, K. L. Griffin, A. E. Hartley, G. Joel, J. Peñuelas, and R. Valentini. 1995. "Relationships between NDVI, Canopy Structure, and Photosynthesis in Three Californian Vegetation Types." *Ecological Applications* 5 (1): 28–41. doi:10.2307/1942049.

Gao, B. 1996. "NDWI - A Normalized Difference Water Index for Remote Sensing of Vegetation Liquid Water from Space." *Remote Sensing of Environment* 58 (3): 257–266. doi:10.1016/S0034-4257(96)00067-3.

Garbulsky, M. F., J. Peñuelas, R. Ogaya, and I. Filella. 2013. "Leaf and Stand-Level Carbon Uptake of a Mediterranean Forest Estimated Using the Satellite-Derived Reflectance Indices EVI and PRI." *International Journal of Remote Sensing* 34 (4): 1282–1296. doi:10.1080/01431161.2012.718457.

Gitelson, A. A., Y. J. Kaufman, R. Stark, and D. Rundquist. 2002. "Novel Algorithms for Remote Estimation of Vegetation Fraction." *Remote Sensing of Environment* 80: 76–87. doi:10.1016/S0034-4257(01)00289-9.

Henry, M. C., and A. S. Hope. 1998. "Monitoring Post-Burn Recovery of Chaparral Vegetation in Southern California Using Multi-Temporal Satellite Data." *International Journal of Remote Sensing* 19 (16): 3097–3107. doi:10.1080/014311698214208.

Hope, A. S., C. Tague, and R. Clark. 2007. "Characterizing Post-Fire Vegetation Recovery of California Chaparral Using TM/ETM+ Time-Series Data." *International Journal of Remote Sensing* 28 (6): 1339–1354. doi:10.1080/01431160600908924.

Huete, A. R. 1988. "A Soil-Adjusted Vegetation Index (SAVI)." *Remote Sensing of Environment* 25 (3): 295–309. doi:10.1016/0034-4257(88)90106-X.

Huete, A. R., K. Didan, T. Miura, E. P. Rodriguez, X. Gao, and L. G. Ferreira. 2002. "Overview of the Radiometric and Biophysical Performance of the MODIS Vegetation Indices." *Remote Sensing of Environment* 83 (1–2): 195–213. doi:10.1016/S0034-4257(02)00096-2.

Hunt, E. R., and B. N. Rock. 1989. "Detection of Changes in Leaf Water Content Using Near- and Middle-Infrared Reflectances." *Remote Sensing of Environment* 30 (1): 43–54. doi:10.1016/0034-4257(89)90046-1.

Jonsson, P., and L. Eklundh. 2004. "TIMESAT- a Program for Analyzing Time-Series of Satellite Sensor Data." *Computers & Geosciences* 30 (8): 833–845. doi:10.1016/j.cageo.2004.05.006.

Keane, R. E., J. K. Agee, P. Z. Fulé, J. E. Keeley, C. H. Key, S. G. Kitchen, R. Miller, and L. A. Schulte. 2008. "Ecological Effects of Large Fires on US Landscapes: Benefit or Catastrophe?" *International Journal of Wildland Fire* 17 (6): 696–712. doi:10.1071/WF07148.

Keeley, J. E., and S. C. Keeley. 1981. "Post-fire regeneration of southern California chaparral." *American Journal of Botany* 68 (4): 524–530. doi:10.2307/2443028.

Keeley, J. E., C. J. Fotheringham, and M. Baer-Keeley. 2005. "Determinants of Postfire Recovery and Succession in Mediterranean-Climate Shrublands of California." *Ecological Applications* 15 (5): 1515–1534. doi:10.1890/04-1005.

Kinoshita, A. M., and T. S. Hogue. 2011. "Spatial and Temporal Controls on Post-Fire Hydrologic Recovery in Southern California Watersheds." *Catena* 87 (2): 240–252. Elsevier B.V doi:10.1016/j.catena.2011.06.005.

Lippitt, C. L., D. A. Stow, J. F. O'Leary, and J. Franklin. 2012. "Influence of Short-Interval Fire Occurrence on Post-Fire Recovery of Fire Prone Shrublands in California, USA." *International Journal of Wildland Fire* 22 (2): 184–193. doi:10.1071/WF10099.

Lu, D. 2006. "The Potential and Challenge of Remote Sensing Based Biomass Estimation." *International Journal of Remote Sensing* 27 (7): 1297–1328. doi:10.1080/01431160500486732.

Malmström, C. M., M. V. Thompson, G. P. Juday, S. O. Los, J. T. Randerson, and C. B. Field. 1997. "Interannual Variation in Global-Scale Net Primary Production: Testing Model Estimates." *Global Biogeochemical Cycles* 11 (3): 367–392. doi:10.1029/97GB01419.

McMichael, C. E., A. S. Hope, D. A. Roberts, and M. R. Anaya. 2004. "Post-Fire Recovery of Leaf Area Index in California Chaparral: A Remote Sensing-Chronosequence Approach." *International Journal of Remote Sensing* 25 (21): 4743–4760. doi:10.1080/01431160410001726067.

Peterson, S. H., D. A. Roberts, and P. E. Dennison. 2008. "Mapping Live Fuel Moisture with MODIS Data: A Multiple Regression Approach." *Remote Sensing of Environment* 112: 4272–4284. doi:10.1016/j.rse.2008.07.012.

Peterson, S. H., and D. A. Stow. 2003. "Using Multiple Image Endmember Spectral Mixture Analysis to Study Chaparral Regrowth in Southern California." *International Journal of Remote Sensing* 24 (22): 4481–4504. doi:10.1080/0143116031000082415.

Prieto, P., J. Peñuelas, J. Llusià, D. Asensio, and M. Estiarte. 2009. "Effects of Experimental Warming and Drought on Biomass Accumulation in a Mediterranean Shrubland." *Plant Ecology* 205 (2): 179–191. doi:10.1007/s11258-009-9608-1.

Riano, D., E. Chuvieco, S. Ustin, R. Zomer, P. Dennison, D. Roberts, and J. Salas. 2002. "Assessment of Vegetation Regeneration after Fire through Multitemporal Analysis of AVIRIS Images in the Santa Monica Mountains." *Remote Sensing of Environment* 79 (1): 60–71. Elsevier doi:10.1016/S0034-4257(01)00239-5.

Riggan, P. J., S. Goode, P. M. Jacks, and R. N. Lockwood. 1988. "Interaction of Fire and Community Development in Chaparral of Southern California." *Ecological Monographs* 58 (3): 155–176. doi:10.2307/2937023.

Rouse, J. W., R. H. Haas, J. A. Schell, and D. W. Deering. 1973. "Monitoring Vegetation Systems in the Great Plains with ERTS." Third ERTS Symposium, NASA SP-351 I, 309–317.

Rundel, P. W., and D. J. Parsons. 1979. "Structural Changes in Chamise (*Adenostoma Fasciculatum*) along a Fire-Induced Age Gradient." *Journal of Range Management* 32 (6): 462–466. doi:10.2307/3898560.

Schmidt, I., J. F. O'Leary, D. A. Stow, K. A. Uyeda, and P. J. Riggan. 2016. "Use of Ultra-High Spatial Resolution Aerial Imagery in the Estimation of Chaparral Wildfire Fuel Loads." *Environmental Monitoring and Assessment* 188: 697. doi:10.1007/s10661-016-5656-x.

Stow, D. A., M. Niphadkar, and J. Kaiser. 2005. "MODIS-Derived Visible Atmospherically Resistant Index for Monitoring Chaparral Moisture Content." *International Journal of Remote Sensing* 26 (17): 3867–3873. doi:10.1080/01431160500185342.

Tague, C., L. Seaby, and A. Hope. 2009. "Modeling the Eco-Hydrologic Response of a Mediterranean Type Ecosystem to the Combined Impacts of Projected Climate Change and Altered Fire Frequencies." *Climatic Change* 93: 137–155. doi:10.1007/s10584-008-9497-7.

Tan, B., C. E. Woodcock, J. Hu, P. Zhang, M. Ozdogan, D. Huang, W. Yang, Y. Knyazikhin, and R. B. Myneni. 2006. "The Impact of Gridding Artifacts on the Local Spatial Properties of MODIS Data: Implications for Validation, Compositing, and Band-To-Band Registration across Resolutions." *Remote Sensing of Environment* 105 (2): 98–114. doi:10.1016/j.rse.2006.06.008.

Uyeda, K. A., D. A. Stow, J. F. O'Leary, I. T. Schmidt, P. J. Riggan. 2016a. "Spatial Variation of Fuel Loading within Varying Aged Stands of Chaparral." In *Applied Vegetation Science*, edited by N. Hölzel, 19 (2): 267–279. doi:10.1111/avsc.12209.

Uyeda, K. A., D. A. Stow, J. F. O'Leary, C. Tague, and P. J. Riggan. 2016b. "Chaparral Growth Ring Analysis as an Indicator of Stand Biomass Development." *International Journal of Wildland Fire* 25: 75–93. doi:10.1071/WF16080.

Uyeda, K. A., D. A. Stow, and P. J. Riggan. 2015. "Tracking MODIS NDVI Time Series to Estimate Fuel Accumulation." *Remote Sensing Letters* 6 (8): 587–596. doi:10.1080/2150704X.2015.1063736.

Van Leeuwen, W. J. D., G. M. Casady, D. G. Neary, S. Bautista, J. A. Alloza, Y. Carmel, L. Wittenberg, D. Malkinson, and B. J. Orr. 2010. "Monitoring Post-Wildfire Vegetation Response with Remotely Sensed Time-Series Data in Spain, USA and Israel." *International Journal of Wildland Fire* 19 (1): 75. doi:10.1071/WF08078.

Wang, J., P. M. Rich, K. P. Price, and W. D. Kettle. 2004. "Relations between NDVI and Tree Productivity in the Central Great Plains." *International Journal of Remote Sensing* 25 (16): 3127–3138. doi:10.1080/0143116032000160499.